

Supporting information

Enhanced Near-Infrared Detection in Organic Phototransistors via Optimized Donor-Acceptor Single-Crystals

Fengzhe Ling, Yanxun Zhang, Qianqian Du,* Xialian Zheng, Qing Liu, Wenjun Wang,* and Shuchao Qin*

School of Physical Science and Information Engineering, Key Laboratory of Optical
Communication Science and Technology of Shandong Province Liaocheng University,
Liaocheng 252059, China

Corresponding Authors

*E-mail: dzdq0126@163.com (Q. Du); lcqinshuchao@126.com (S. Qin);
phywwang@163.com

S1. Preparation of doped crystal

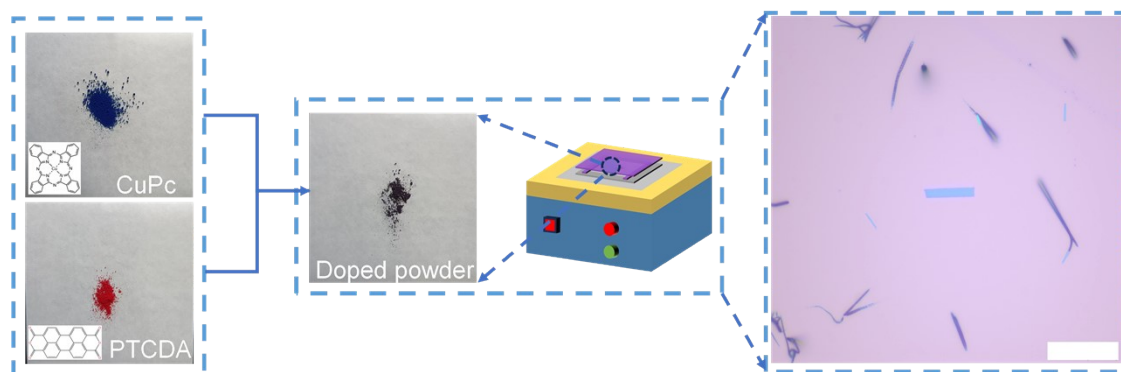


Figure S1. The process diagram of synthesis of the doped crystal sample prepared by micro-spacing air sublimation method.

Sample preparation process: Firstly, two materials of different concentrations of CuPc (blue) and PTCDA (red) are fully mixed by grinding method, then the final mixed powder (black) is placed on the heating table to obtain high-quality single crystals.

S2. The infrared (NIR) absorption spectrum of the CuPc, PTCDA and PTCDA doped CuPc crystal

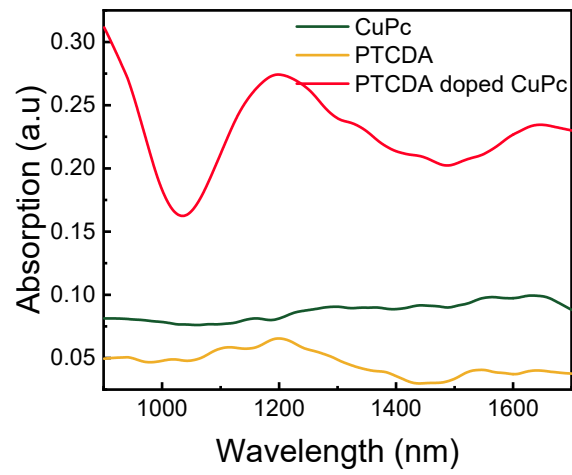


Figure S2. The infrared absorption (Abs) spectra of the CuPc, PTCDA and PTCDA doped CuPc crystal.

S3. Transfer curves and responsivity of the doped crystal

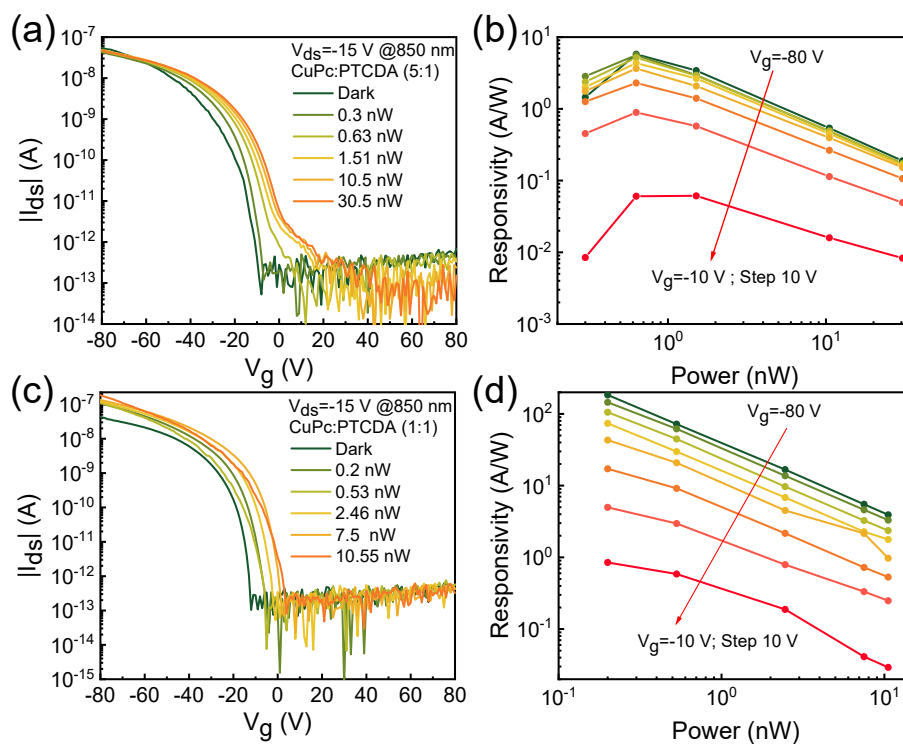


Figure S3. (a) Transfer characteristics curves of doped crystal (CuPc:PTCDA=5:1) without illumination and under different light illumination (850 nm), at $V_{ds} = -15$ V. (b) Responsivity of this device calculated from transfer curves. (c) Transfer curves of doped crystal (CuPc:PTCDA=1:1), at $V_{ds} = -15$ V. (d) The corresponding responsivity of this device.

S4. The noise current spectral density

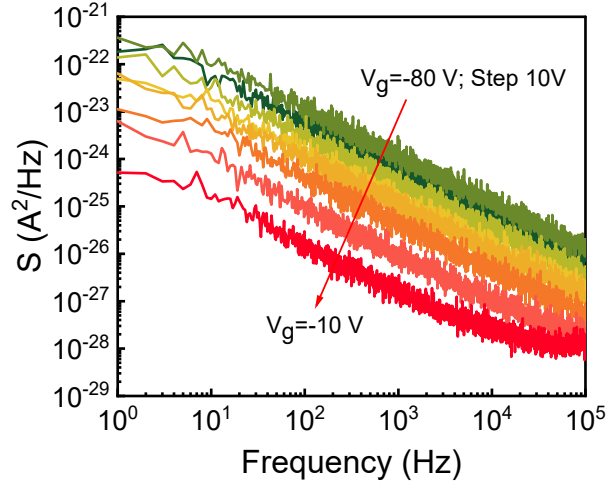


Figure S4. Noise current spectral density of the device as a function of the frequency under different gate biases.

D^* can be expressed as $D^* \approx \frac{RA^{1/2}}{\sqrt{S(f)}}$, where NEP is noise equivalent power

$NEP = \frac{\sqrt{\langle i_n^2 \rangle} / \Delta f}{R}$ (units $W Hz^{-1/2}$) and Δf is the electrical bandwidth set to be 1 Hz. We

carried out spectral noise density with different gate voltages from -80 to -10 V with a step size of 10 V (Figure S3), to analyze the noise current $\langle i_n^2 \rangle = \int_0^{\Delta f} S(f) df$. At smaller

measurement bandwidths of $\Delta f = 1$, the specific detectivity D^* can be reduced to

$$D^* = \frac{RA^{1/2}}{\sqrt{\int_0^{\Delta f} S(f) df / \Delta f}} \approx \frac{RA^{1/2}}{\sqrt{S(f)}}$$

S5. The transient photoresponse of the doped crystals

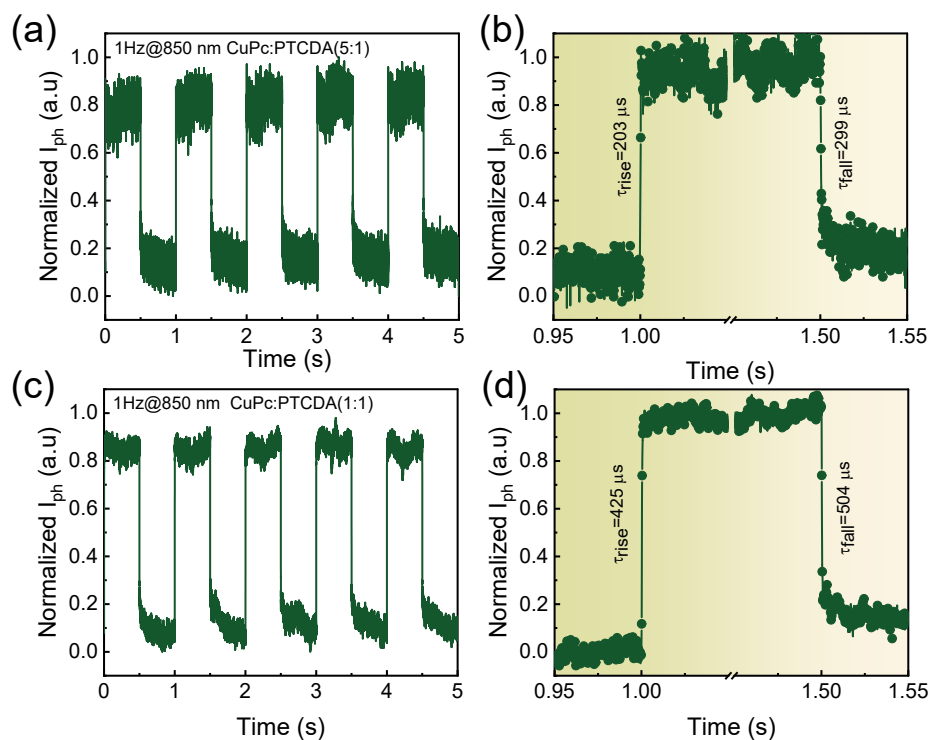


Figure S5. (a) The transient photoresponse of a typical doped devices with CuPc:PTCDA=5:1. (b) The τ_{rise} and τ_{fall} from an amplifying transient cycle. (c) The transient photoresponse of a typical doped devices with CuPc:PTCDA=1:1. (d) The τ_{rise} and τ_{fall} from an amplifying transient cycle.

S6. AFM roughness and potential of the doped crystals

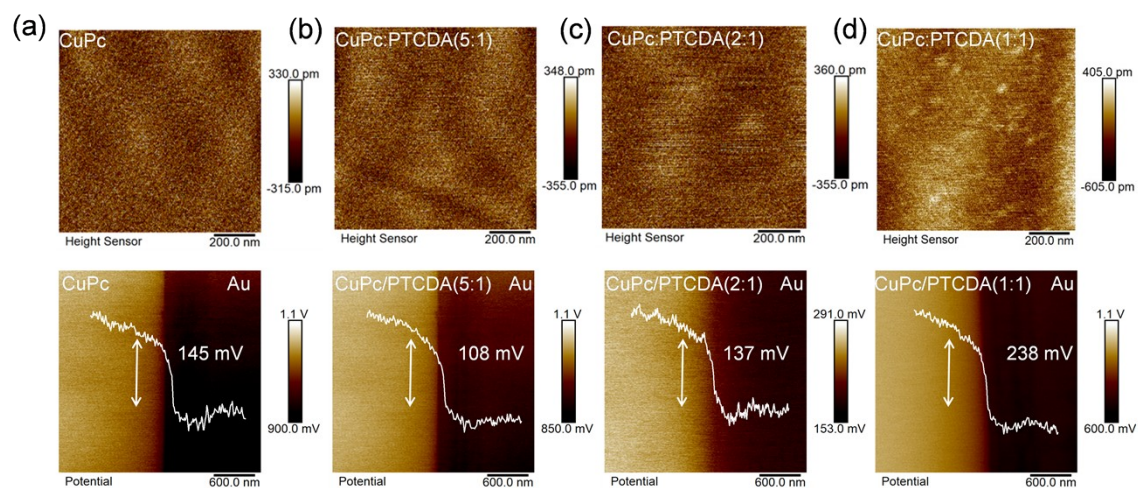


Figure S6. AFM roughness and potential of isolated CuPc (a), doped crystals with different mole ratio (b-d).

S7. The broad spectrum photoresponse of the doped crystals

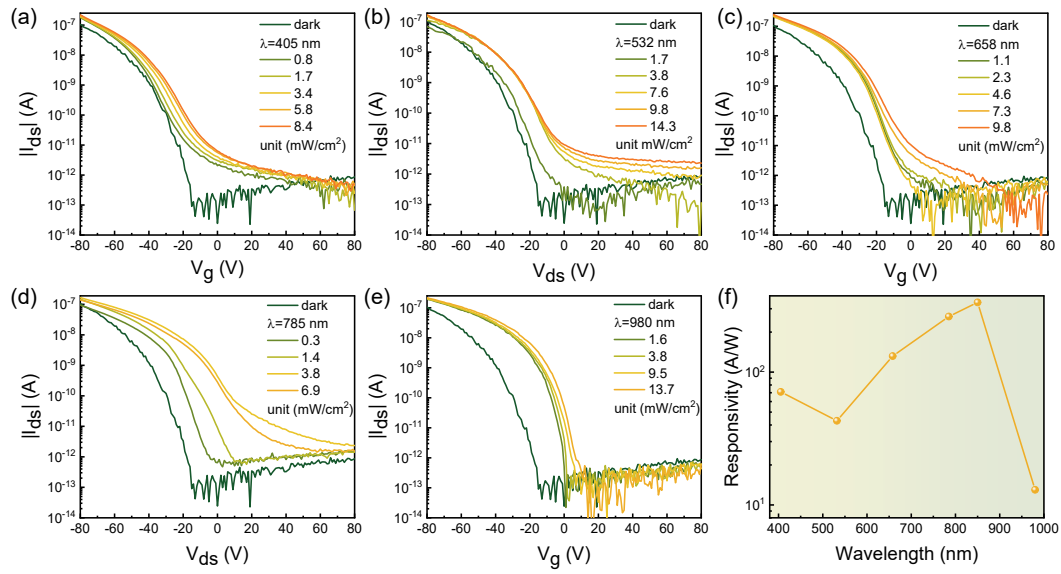


Figure S7. (a-g). The transfer curve of the device for various illumination wavelengths (405, 532, 658, 785, and 980 nm). (f). The responsivity of the device for different incident wavelengths.